Molecular Modelling Guided Experimental Study for Isotopic Enrichment of Gadolinium

A. Boda, S.K. Arora, A.K. Singha Deb, J.M. Joshi, M. Jha, S. Govalkar, P.V. Kadale, Sk. M. Ali, S. Mukhopadhyay and K.T. Shenoy
Chemical Engineering Division

Abstract

Molecular modelling and experimental studies were performed to predict the feasibility of Gd isotope separation using crown ether grafted resin. BP and B3LYP functional - based DFT calculations foretell the complexation stability order of Gd^{3+} ion as DCH18C6>B15C5>DB18C6 as observed in the experiment. The calculated isotopic separation factor shows that DB18C6 is the promising candidate. Hence, CMPS grafted DB18C6 resin was chosen for the isotope separation of Gd. The adsorption capacity of the resin for Gd^{3+} ion was found to be 1mg/g. The separation coefficients ($\varepsilon \times 10^3$) were found to be 6.3, 3.4, 9.7 and 11.1 for the isotopic pair of 155/158, 157/158, 155/160 and 157/160 respectively and shows promise for future study.

Introduction

Naturally occurring gadolinium (Gd) consists of 7 stable isotopes. ^{152}Gd, ^{154}Gd, ^{155}Gd, ^{156}Gd, ^{157}Gd, ^{158}Gd and ^{160}Gd of which abundance ratios are 0.20, 2.18, 14.80, 20.47, 15.65, 24.84 and 21.86 at%, respectively [1]. Gadolinium has the highest cross section for the capture of thermal neutrons compared to other elements. Further, ^{157}Gd and ^{155}Gd have the higher cross sections of 254000 and 60900 barns respectively compared to the remaining isotopes of Gd. Natural Gd is currently used as a burnable poison in nuclear fuel but the use of only Gd-155/157 has been proposed as this would create an even more effective burnable poison [2].

The three main methods for the production of stable isotopes are: distillation [3], centrifuge [4] and electromagnetic separation [5, 6] (calutron), but each of these methods has its own limitations. The chemical exchange isotope separations, on the other hand, have usually small separation coefficients and necessitate a longer time duration to obtain enriched products; however chemical exchange isotope separations are inherently equilibrium processes and are therefore considered as energy conservation processes. Separation of isotopes by chromatography is one of the most effective chemical exchange methods, which is based on the chemical equilibrium between isotopic species distributed between the stationary phase and mobile solution phase. It has been applied successfully to the separation of isotopes of various elements of lower mass [7-14].

Because crown ethers are good complex forming compounds for most of the metal ions, isotope separations are obviously best investigated by means of chemical reactions with crown ethers [15-17]. The separation of isotopes using dibenzo- and dicyclohexyl-18-crown-6 [18] was first demonstrated by Jepson et al. [18]. Because of high isotopic separation factors with crown ethers, they are recently being used as promising isotope enrichment agents [19].

The application of molecular modelling is growing rapidly with continuing developments in computer power, robust algorithms, and availability of software. Today molecular modelling can sometimes provide useful estimates of the properties and behavior of materials, even before they have been synthesized and it also provides useful estimates of the parameters needed for traditional chemical engineering process development & design. Development of suitable adsorbents for the separation of isotopes by means of experiment alone is a difficult task which can be made little easier by predicting the enrichment factor for the elements of interest employing molecular modelling [20-24]. The present work reports the molecular modelling and experimental study to predict the feasibility of Gd isotope separation using Chloromethylated polystyrene (CMPS) grafted DB18C6 crown ether resin.

Molecular modelling

Isotope effect is a quantum mechanical phenomenon and hence it is obvious to study the isotope effect of

gadolinium using quantum computation-based molecular modelling.

Computational protocol

All the geometries of the free as well as complexes are optimized using Turbomole[25] package at BP86/SV(P) level of theory[26]. Single point energy calculations were carried out on optimized complexes at B3LYP/TZVP [27, 28] level. The optimized structures of different chemical species are drawn using MOLDEN molecular visualization graphics programme. The binding energies (ΔE) are calculated for the complexation of metal ions (M) with ligands (L): M + L = ML as given below,

$$\Delta E = E_{ML} - (E_M + E_L) \qquad (1)$$

Here E_{ML}, E_M and E_L are the energies of the molecular complex, metal ion and ligand respectively. The selectivity of the crown ether is demonstrated by the calculated values of ΔE of Gd^{3+} ion with the ligands.

Theory

Isotope effects in chemical exchange reactions are mainly quantum mechanical and hence cannot be explained by classical statistical mechanics. Quantum electronic structure theory based computational methods are becoming increasingly central to understanding the fractionation of stable isotopes in various chemical exchange systems. The equilibrium constants for isotopic exchange reactions from spectroscopic data was reported by Urey et al.[29]. The separation factor for the following isotopic exchange reaction

$$^zM^{+3}_{aq.} + {}^{z+\Delta m}M^{+3}_{compl} \leftrightarrow {}^{z+\Delta m}M^{+3}_{aq.} + {}^zM^{+3}_{compl} . \qquad (2)$$
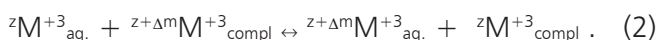
z = atomic mass and M^{+3} = metal ion. (compl means complexed by the ligand) can be written in terms of reduced partition function ratio (RPFR, f ^{r}) as [30]

$$\alpha = f\, {}^rM^{+3}_{aq.} / f\, {}^rM^{+3}_{compl} \qquad (3)$$

f^r is given by

$$f^r = Z_{vib}{}^{z+\Delta m}M^{+3}\Pi_i(h\nu_i{}^{z+\Delta m}M^{+3}/k_BT)/Z_{vib}{}^zM^{+3}\Pi_i(h\nu_i{}^zM^{+3}/k_BT) \qquad (4)$$

Here, Z and n are the vibrational partition function and frequency, k_B and h are the Boltzmann and Planck constants respectively and T is the temperature. The main input required for the evaluation of RPFR and separation factor is the harmonic vibrational frequency of the system of interest.
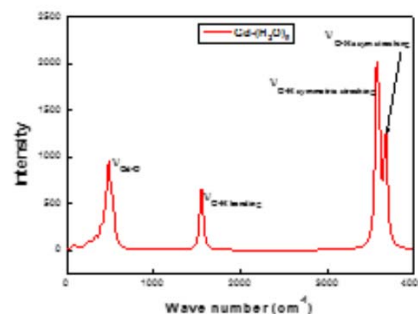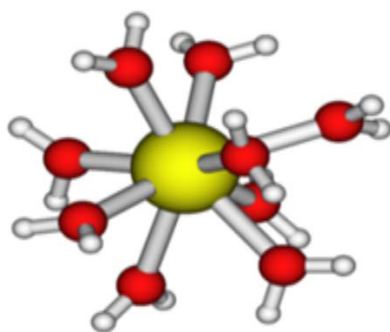

Fig. 1: Optimized geometry of hydrated Gd^{3+} ion and calculated IR spectra

Results and Discussion

Molecular Modelling

Most of the isotopic enrichment of the elements takes place from aqueous feed solution. Therefore, it is of primary importance to understand the hydration sphere structure of the metal ion of interest. For any quantum computation, the structure of the system under study has to be considered first. The nonahydrated structure of Gd^{3+} ion has been reported earlier using EXAFS [31]. Hence, we have considered nona-hydrated cluster of Gd^{3+} ion instead of searching for all possible structures. The structure of ($Gd^{3+}(H_2O)_9$) is displayed in Fig. 1.

The calculated Gd-O distance (2.52) is found to be well matched with the EXAFS data (2.39)[31]. The corresponding IR frequency is also presented in Fig.1. The first peak arises due to the Gd-O bond and the remaining three are the signatures of bending, symmetric and anti symmetric stretching of O-H bond respectively. Three crown ethers namely DCH18C6, B15C5 and DB18C6 were used in the complexation studies of Gd^{3+} ion. The optimized structures of B15C5, DB18C6 and DCH18C6 and their complexes with Gd^{3+} ion are given in Fig.2. The reported ionic radii of Gd^{3+} ion is 2.16 . From the structural parameters it is found that the metal ion oxygen bond distance is found to be smaller in case B15C5 (2.368) as compared to DCH18C6 (2.402) and DB18C6 (2.625). Furthermore, the position of Gd^{3+} ion with respect to mean plane is displayed in Fig.2.

The calculated ΔE and ΔG of Gd^{3+} ion with the crown ethers both in gas and solvent phases are given in Table.1. The ΔE shows the order DCH18C6>DB18C6>B15C5. The ΔG in the gas phase also portrays similar trend of binding. Meanwhile, solvent phase calculations show the order DCH18C6>B15C5> DB18C6. This is because the solvation free energy of B15C5-Gd^{3+} complex is much
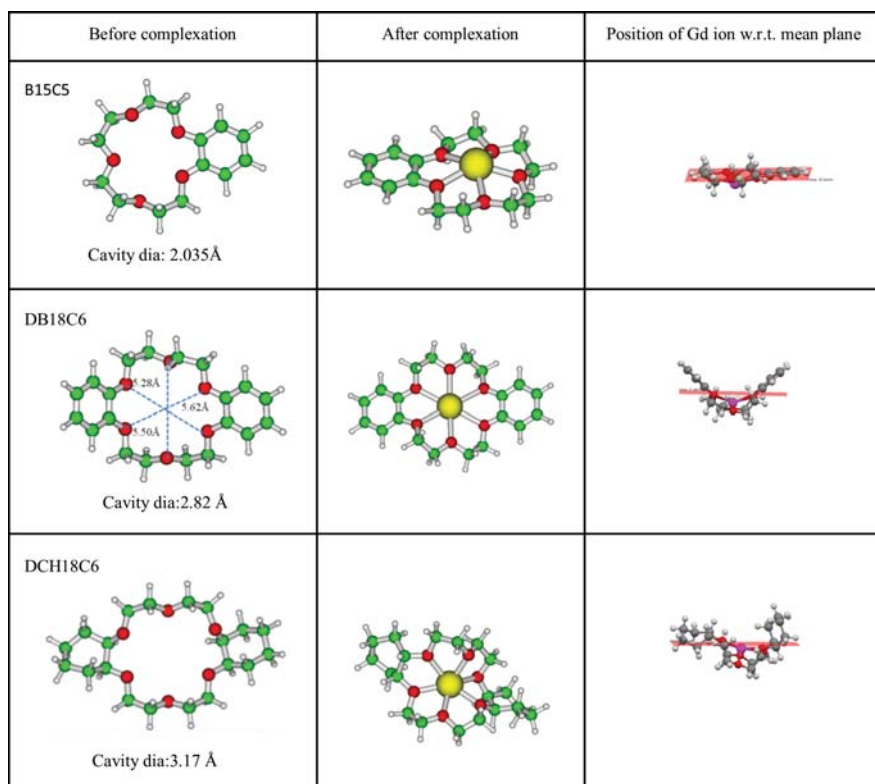
Before complexation	After complexation	Position of Gd ion w.r.t. mean plane
B15C5 Cavity dia: 2.035Å		
DB18C6 Cavity dia:2.82 Å		
DCH18C6 Cavity dia:3.17 Å		

Fig. 2: Optimized structures of B15C5, DB18C6 and DCH18C6 and their complexes with Gd^{3+} ion

higher than DB18C6-Gd^{3+}. However, DCH18C6 was found to have more free energy of extraction.

The RPFR of Gd isotopic pair of 155/160 was found to be higher than 157/160 pair as shown in Table 2. The values of RPFR and α for hydrated Gd^{3+} ion and complexes of Gd^{3+} with various crown ligands were computed. In the case of dowex resin, observed separation factors are 1.000102 and 1.000086 for isotopic pairs of 155/160 and 157/160 respectively which are close to the experimental values of 1.000064 and 1.000040[11]. The separation factor for 155/160 pair is found to be higher compared to the 157/160 pair, due to a larger mass difference (Δm) in the case of 155/160 pair. The results show that α value with DB18C6 is higher compared to B15C5, DCH18C6. In view of comparatively higher α, DB18C6

is considered to be promising for enrichment. But, in order to get considerable amount of enriched isotopes, the ligand should be grafted on solid matrix and then the separation should be carried out in columnar mode. To meet these criteria, DB18C6 is grafted on CMPS resin. In order to keep the molecular system computationally tractable, only one DB18C6 was anchored on repeated monomeric unit of CMPS. The optimized structure of Gd^{3+}-CMPS-DB18C6 is displayed in Fig.3. The predictability of computational protocol was validated by using the reported results of commercially available dowex resin with EDTA as complexing/enrichment agent. Furthermore, the calculated separation factor for 152/160 pair for Gd^{3+}-DCH18C6 (α=1.0012) was found to be in good agreement with the experimental results (α=1.002)[32] and thus confirms the acceptability of the present method of computation.

Experiments

Separation of Gadolinium Isotopes Using Solvent Extraction

$GdCl_3$ solution (0.03M) was used as the aqueous phase. The organic phase was 0.1M solution of B15C5, DB18C6 and DCH18C6 in nitrobenzene. 5 mL of each was mixed and then stirred for 1 hr in a magnetic stirrer. They were then allowed to stand for a day. The supernatant solution was used for concentration measurement. The concentration was determined by using ICP-MS and isotopic analysis was carried out using TIMS, developed by the Technical Physics Division, BARC. The distribution coefficient (K_d) of

Table 1: ΔE and ΔG of Gd^{3+} ion towards crown ethers and NBO charges on metal ion

|	Gd^{3+}-B15C5	Gd^{3+}-DB18C6	Gd^{3+}-DCH18C6
Charge on metal ion(gas)	2.098	1.651	2.110
Charge on metal ion(sol)	2.421	1.704	2.241
E(gas) (kJ/mol)	-1503.21	-1641.73	-1640.89
ΔG (gas) (kJ/mol)	-1454.96	-1590.01	-1603.57
ΔE (NB) (kJ/mol)	-122.87	-49.32	-124.72
ΔG (NB) (kJ/mol)	-74.62	2.40	-87.40
ΔS (kJ/mol K)	-0.145	-0.170	-0.141
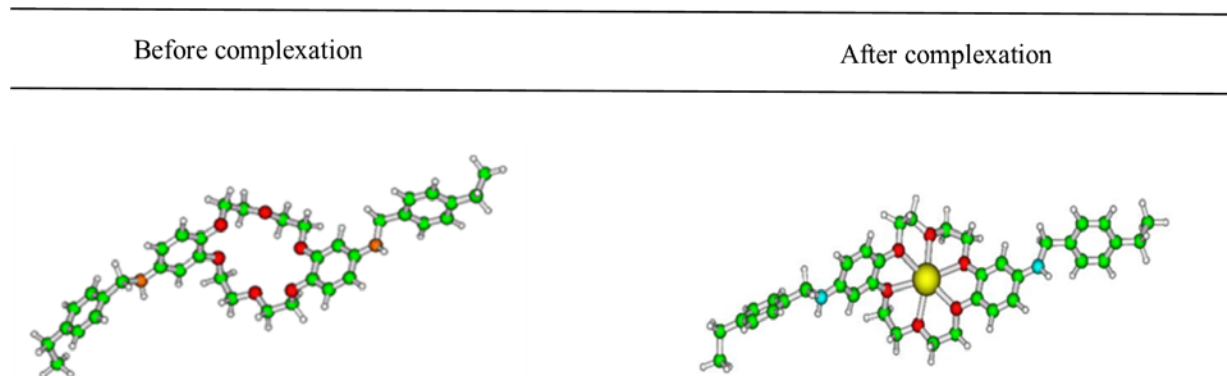
Fig. 3: Optimized structures of complex of DB18C6 grafted CMPS with Gd³⁺ ion

metal ion, between organic and aqueous solution was determined using the following equation:

$$K_d = \frac{C_i - C_f}{C_f} \qquad (5)$$

Where C_i and C_f are the tinitial feed and final supernatant concentration of Gd³⁺ ion.

From Fig.4, it is found that the K_d value of Gd³⁺ follows the order DCH18C6 > B15C5 > DB18C6. From the molecular modelling calculations also, the same trend has been observed which further validates the computational results. So the present study thus validates the importance of computational study which can be used to elucidate the underlying mechanism for the metal ion selectivity (based only on theoretical route) and thus contributes to the design and screening of suitable ligands using computations. Although DB18C6 shows positive free energy from Quantum mechanics calculation, the experiments show the reverse picture. This anomaly may be addressed by appropriate consideration of spin state of the chemical species. The separation factor with DB18C6 was found to be higher compared to B15C5, DCH18C6 and also EDTA which shows that the use DB18C6 will be promising for future studies. So based on this, DB18C6 grafted to CMPS resin was synthesized in our lab and used for the isotope separation.
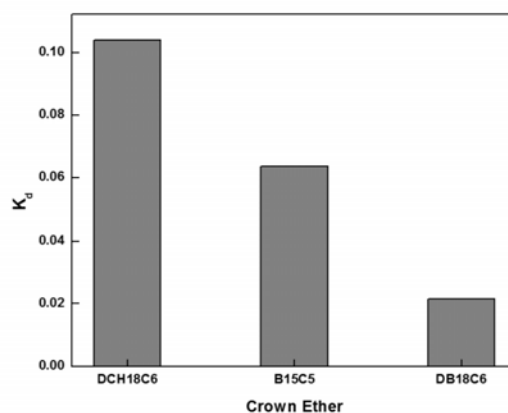
**Fig. 4: K_d values of B15C5, DB18C6 and DCH18C6 in nitrobenzene**

Distribution Coefficient Using Grafted Resin in Batch Method

The distribution coefficient (K_d) was evaluated using batch method. Each portion of 0.1g of dry (regenerated) CMPS grafted DB18C6 resin was weighed accurately and transferred into 50ml PP bottle. Then 10ml of Gd(NO₃)₃ solution of varying concentrations (100ppm to 200ppm) was added. The solutions were subjected to manual shaking at regular interval for 30min and kept overnight. The concentration of Gd³⁺ ion in the supernatant solutions

Table 2: RPFR and separation factor of Gd in water, EDTA and crown ether complexes

Complex of Gd³⁺	RPFR(f)		á$_{155/160}$ =f$_{aq}$/f$_{comp}$	á$_{157/160}$ =f$_{aq}$/f$_{comp}$
	Gd$_{155/160}$	Gd$_{157/160}$		
9w	1.0024	1.0014		
EDTA	1.00151	1.000914	1.000102 (1.000064)	1.000086 (1.000040)
DCH18C6	1.001890	1.001083	1.000509	1.000317
DB18C6	1.000647	1.000391	1.001752	1.001009
B15C5	1.002016	1.001213	1.000383	1.000187
CMPS-DB18C6	1.001191	1.000712	1.0012	1.00068
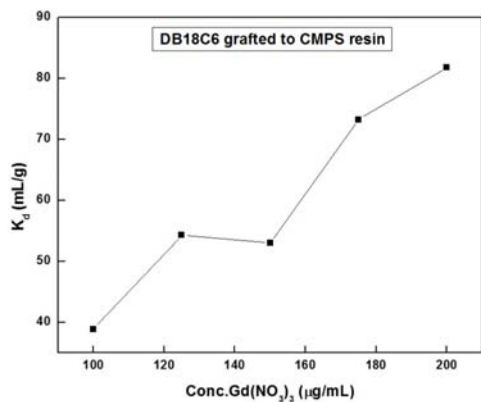
Fig. 5: K_d values versus concentration of Gd³⁺ ion in separation with CMPS-DB18C6 resin

was determined using ICP-MS. The K_d of metal ion, between resin and solution, was determined using the following equation:

$$K_d = \left[\frac{C_i - C_f}{C_f} \right] \times \frac{V}{M} \, (ml/g) \qquad (6)$$

Where C_i = initial concentration of the solution, C_f = concentration of the supernatant solution, V = total volume of the solution (ml) and M = mass of dry resin (g).

The K_d values are plotted in Fig.5 indicating that the K_d value increases on increasing the concentration of metal ion with the resin.

Separation of Gadolinium Isotopes Using Column Chromatography

A breakthrough experiment was conducted in 6mm dia and 1m length column with CMPS-DB18C6 resin for Gd³⁺ ion using 0.005M Gd(NO₃)₃ (800ppm) at pH 6.50. The loaded Gd³⁺ was eluted using 0.5M HCl. The breakthrough curve is displayed in Fig.6a. From the breakthrough experiment it is observed that the adsorption capacity for Gd³⁺ ion is ∼1mg/gm of resin.

Breakthrough curve indicates that the leakage of Gd³⁺ starts after volume reaches around 25 ml.

A study was also conducted by connecting two columns each of 6mm dia and 1m length column in series with CMPS-DB18C6 resin (Fig.7) for Gd³⁺ ion using 0.005M Gd(NO₃)₃. The pH was adjusted with NH₄OH to 6.50. The excess amount of Gd³⁺ was passed continuously to check the feasibility of isotope exchange. Samples were collected after every 20.0 ml turn, using automatic fraction collector, (Buchi make, Switzerland). The concentration of the samples was analyzed using ICP-MS and isotopic analysis of last few samples was carried out using TIMS. The loaded Gd³⁺ ion is further eluted using 0.5M HCl. The breakthrough curve is displayed in Fig.6b. The
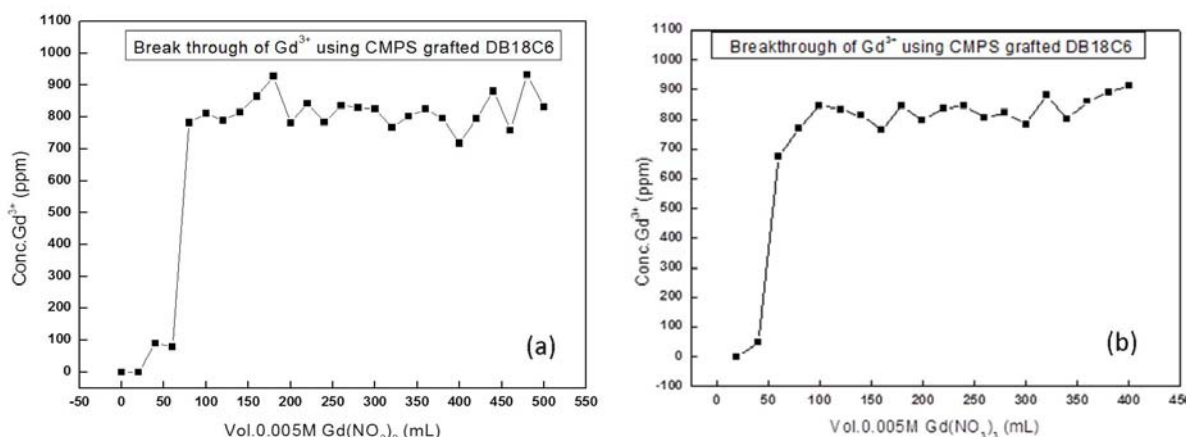

Fig.7: Experimental setup of chromatographic separation of Gd isotopes

estimated values of isotope composition are presented in Tables 3 and 4.

The single stage separation factor, $\alpha = 1 + \varepsilon$ for each Gd isotope to defined as

$$\alpha = \frac{\left[\dfrac{^L Gd}{^H Gd} \right]_{resin}}{\left[\dfrac{^L Gd}{^H Gd} \right]_{sol}} \qquad (7)$$

Fig. 6: Breakthrough experiment using CMPS-DB18C6 resin for Gd³⁺ ion (a) Single column (b) double column

Table 3: The Gd isotopic ratios of samples collected in break through

Sample	Gd-155/158	Gd-157/158	Gd-155/160	Gd-157/160
Natural	0.59742±0.04%	0.63212±0.05%	0.67845±0.04%	0.71786±0.03%
B16	0.59940±0.03%	0.63410±0.02%	0.67786±0.03%	0.71710±0.02%
B18	0.59670±0.01%	0.63220±0.02%	0.67445±0.05%	0.71458±0.02%
B19	0.59831±0.03%	0.63236±0.01%	0.67695±0.01%	0.71547±0.01%
B20	0.59766±0.03%	0.61782±0.02%	0.67503±0.03%	0.69780±0.08%

Table 4: The Gd isotopic ratios of samples collected by eluting with HCl of sorbed Gadolinium

Sample	Gd-155/158	Gd-157/158	Gd-155/160	Gd-157/160
E1	0.59721±0.09%	0.631699±0.1%	0.67546±0.1%	0.71447±0.1%
E2	0.601814±0.002%	0.615184±0.1%	0.68576±0.5%	0.70100±0.5%
E4	0.5951±0.015%	0.631140.026%	0.67224±0.02%	0.71295±0.03%
E7	0.601023±0.02%	0.636394±0.1%	0.67879±0.04%	0.71874±0.1%

The separation coefficients, ε was calculated by using the isotopic enrichment curves of the front and rear boundaries according to the following equation [33].

$$\varepsilon = \sum \left(\frac{q_j}{QR_0} \right) \left[\frac{R_j - R_0}{1 - R_0} \right] \qquad (8)$$

where q is the amount of Gd in the sample fraction, Q is the total amount of sorbed Gd in the column packed resin, R_j is the isotopic ratio of $^LGd/^HGd$, and the subscripts j and o denote the fraction number and the original feed, respectively. In general, the isotope exchange reaction effectively proceeds and reaches the equilibrium between two phases of the solution and the resin at lower flow rate condition.

From the isotopic values in Table 3 the isotope separation coefficient was calculated. The separation coefficients, $\varepsilon \times 10^3$, were found to be 6.3, 8.9, 3.4, 9.7, 11.1 and 32.4 for 155/158, 156/158, 157/158, 155/160, 157/160 and 158/160 pairs respectively.

From the isotopic ratio measurements it was observed that slight isotopic separations have taken place in the resin bed. Since the adsorption capacity is low, more material is needed for the achievement of higher separation. Further study is in progress.

Conclusions

A combined molecular modelling and experimental study was performed for the feasibility of Gd isotope separation using crown ether functionalized resin. From the quantum calculations it was observed that the complexation of Gd^{3+} shows the order DCH18C6>B15C5> DB18C6 which was verified by performing a solvent extraction experiment. The calculated isotopic separation factor values show that DB18C6 is a promising candidate. So, CMPS-DB18C6 resin was chosen for the preliminary study of Gd isotopic separation. The adsorption capacity of the resin for Gd^{3+} was found to be 1mg/g. The separation coefficients ($\varepsilon \times 10^3$) were found to be 6.3, 3.4, 9.7 and 11.1 for 155/158, 157/158, 155/160 and 157/160 respectively and show promise for further study.

References

[1]   Berglund, M., Wieser, M. E., *Pure and Applied Chemistry* 2009, *83*, 397-410.

[2]   Sears, V. F., *Thermal-neutron scattering lengths and cross sections for condensed-matter research*, Chalk River Nuclear Laboratories Chalk River (Ontario) 1984.

[3]   Abdollahi, M., Ahmadi, S. J., *Chemical Engineering and Processing: Process Intensification* 2014, *76*, 26-32.

[4]   Artyukhov, A. A., Babichev, A. P., Knyasev, I. Y., Kravets, Y. M., *et al.*, *Nuclear Instruments and Methods in Physics Research Section A: Accelerators, Spectrometers, Detectors and Associated Equipment* 1997, *401*, 281-288.

[5]   Egle, B. J., Hart, K. J., Aaron, W. S., *Journal of Radioanalytical and Nuclear Chemistry* 2014, *299*, 995-999.

[6]   Keim, C. P., *Annual review of nuclear science* 1952, *1*, 263-292.

[7]   Chen, J., Nomura, M., Fujii, Y., Kawakami, F., Okamoto, M., *Journal of Nuclear Science and Technology* 1992, *29*, 1086-1092.

[8]   Hagiwara, Z., *Journal of Nuclear Science and Technology* 1969, *6*, 508-513.

[9]　Ismail, I., Matin, M., Nomura, M., Begum, S., Fujii, Y., *J. Ion Exch.* 2002, *13*, 40-45.

[10]　Ismail, I., Nomura, M., Fujii, Y., *Journal of Nuclear Science and Technology* 1998, *35*, 801-807.

[11]　Ismail, I. M., Fukami, A., Nomura, M., Fujii, Y., *Analytical Chemistry* 2000, *72*, 2841-2845.

[12]　Ismail, I. M., Nomura, M., Fujii, Y., *Journal of Chromatography A* 1998, *808*, 185-191.

[13]　Zhang, Y. H., Gunji, S., Nomura, M., Fujii, Y., Oi, T., *Journal of Chromatography A* 2005, *1069*, 133-139.

[14]　Zhang, Y. H., Nomura, M., Aida, M., Fujii, Y., *Journal of Chromatography A* 2003, *989*, 175-182.

[15]　Lehn, J. M., Sauvage, J. P., *Journal of the American Chemical Society* 1975, *97*, 6700-6707.

[16]　Christensen, J. J., Eatough, D. J., Izatt, R. M., *Rev* 1974, *74*, 351.

[17]　VAgtle, F., Weber, E., *Angew. Chem* 1974, *86*, 727.

[18]　Jepson, B. E., DeWitt, R., *Journal of Inorganic and Nuclear Chemistry* 1976, *38*, 1175-1177.

[19]　Heumann, K. G., *Organic Chemistry*, Springer 1985, pp. 77-132.

[20]　Ali, S. M., Boda, A., Shenoy, K. T., Shenoi, M. R. K., *et al.*, *BARC Report* 2012, *R/005*, 1-60.

[21]　Boda, A., Ali, S. M., Shenoi, M. R. K., Rao, H., Ghosh, S. K., *BARC REPORT* 2011, *I/011*, 1-24.

[22]　Arora, S. K., Boda, A., Joshi, J. M., Singha Deb, A. K., *et al.*, *Proceedings of the DAE-BRNS biennial symposium on emerging trends in separation science and technology* 2014.

[23]　Boda, A., Singha Deb, A. K., Ali, S. M., Shenoy, K. T., Ghosh, S. K., *American Institute of Physics Conference Series* 2014, pp. 1065-1067.

[24]　Singha Deb, A. K., Ali, S. M., Shenoy, K. T., Ghosh, S. K., *Journal of Chemical & Engineering Data* 2014, *59*, 2472-2484.

[25]　Ahlrichs, R., Bar, M., Haser, M., Horn, H., Kolmel, C., *Chem. Phys. Letters* 1989, *162*, 165.

[26]　Becke, A. D., *Physical Review A* 1988, *38*, 3098.

[27]　Becke, A. D., *The Journal of Chemical Physics* 1993, *98*, 1372-1377.

[28]　Lee, C., Yang, W., Parr, R. G., *Physical Review B* 1988, *37*, 785.

[29]　Urey, H. C., Rittenberg, D., *The Journal of Chemical Physics* 1933, *1*, 137-143.

[30]　Bigeleisen, J., *Journal of the American Chemical Society* 1996, *118*, 3676-3680.

[31]　Persson, I., D'Angelo, P., De Panfilis, S., SandstrAm, M., Eriksson, L., *Chemistry-A European Journal* 2008, *14*, 3056-3066.

[32]　Fujii, T., Yamamoto, T., Inagawa, J., Gunji, K., *et al.*, *Solvent extraction and ion exchange* 1999, *17*, 1219-1229.

[33]　Spedding, F. H., Powell, T. E., Svec, H. J., *Journal of the American Chemical Society* 1955, *77*, 6125-6132.